Error-free demodulation of pixelated carrier frequency interferograms

M. Servin* and J. C. Estrada,

[1]*Centro de Investigaciones en Optica A.C., Loma del Bosque 115, 37150 Leon Guanajuato, Mexico*
**mservin@cio.mx*

Abstract: Recently, pixelated spatial carrier interferograms have been used in optical metrology and are an industry standard nowadays. The main feature of these interferometers is that each pixel over the video camera may be phase-modulated by any (however fixed) desired angle within $[0,2\pi]$ radians. The phase at each pixel is shifted without cross-talking from their immediate neighborhoods. This has opened new possibilities for experimental spatial wavefront modulation not dreamed before, because we are no longer constrained to introduce a spatial-carrier using a tilted plane. Any useful mathematical model to phase-modulate the testing wavefront in a pixel-wise basis can be used. However we are nowadays faced with the problem that these pixelated interferograms have not been correctly demodulated to obtain an error-free (exact) wavefront estimation. The purpose of this paper is to offer the general theory that allows one to demodulate, in an exact way, pixelated spatial-carrier interferograms modulated by any thinkable two-dimensional phase carrier.

OCIS codes: (120.3180) Interferometry; (120.2650) Fringe Analysis.

References and links

1. D. Malacara, M. Servin, and Z. Malacara, *Interferogram Analysis for Optical Testing*, 2 ed., (Taylor & Francis Group, CRC Press, 2005).
2. M. Takeda, H. Ina, and S. Kobayashi, "Fourier-transform method of fringe-pattern analysis for computer-based topography and interferometry," J. Opt. Soc. Am. A **72**(1), 156–160 (1982).
3. R. Smythe, and R. Moore, "Instantaneous phase measuring interferometry," Opt. Eng. **23**, 361–364 (1984).
4. O. Y. Kwon, "Multichannel phase-shifted interferometer," Opt. Lett. **9**(2), 59–61 (1984).
5. C. L. Koliopoulos, "Simultaneous phase-shift interferometer," Proc. SPIE **1531**, 119–127 (1992).
6. B. K. A. Ngoi, K. Venkatakrishnan, and N. R. Sivakumar, "Phase-shifting interferometry immune to vibration," Appl. Opt. **40**(19), 3211–3214 (2001).
7. J. Millerd, N. Brock, J. Hayes, M. North-Morris, M. Novak, and J. C. Wyant, "Pixelated phase-mask dynamic interferometer," Proc. SPIE **5531**, 304–314 (2004).
8. M. Novak, J. Millerd, N. Brock, M. North-Morris, J. Hayes, and J. Wyant, "Analysis of a micropolarizer array-based simultaneous phase-shifting interferometer," Appl. Opt. **44**(32), 6861–6868 (2005).
9. J. F. Mosiño, M. Servin, J. C. Estrada, and J. A. Quiroga, "Phasorial analysis of detuning error in temporal phase shifting algorithms," Opt. Express **17**(7), 5618–5623 (2009).
10. B. T. Kimbrough, "Pixelated mask spatial carrier phase shifting interferometry algorithms and associated errors," Appl. Opt. **45**(19), 4554–4562 (2006).

1. Introduction

The spatial phase modulation technique that uses a tilted plane reference is well known and useful technique to demodulate the measuring wavefront in an interferometer [1]. In this way one obtains the following spatial carrier interferogram,

$$I(x,y) = a(x,y) + b(x,y)\cos[\varphi(x,y) + \omega_x\, x + \omega_y\, y]. \qquad (1)$$

Where $I(x,y)$ is the interferogram's intensity as imaged over the CCD video camera. The functions $\phi(x,y)$, $a(x,y)$ and $b(x,y)$ are respectively the searched phase, the background illumination and the amplitude of the fringe pattern. Finally ω_x and ω_x are two constants proportional to the slope of the reference tilted plane. There are at least two ways of analyzing

#130068 - $15.00 USD Received 14 Jun 2010; revised 10 Jul 2010; accepted 10 Jul 2010; published 13 Aug 2010

these carrier interferograms; spatial phase-shifting techniques [1], and the Fourier transform based ones [2]. The main motivation behind spatial phase modulation is to measure a wavefront's phase in hostile mechanical environments where the use of temporal phase shifting interferometry may be impossible [3–6].

Recently a very clever spatial carrier modulation technique that uses pixelated phase-shift was developed [7,8]. In this experimental approach one is totally free to define the mathematical form of the phase carrier. The only limitation is that the modulating phase-mask remains fixed, placed before the CCD light sensor [7,8]. A reasonable way to formally express a pixelated carrier interferogram modulated by $pm(x,y)$ is,

$$I(x, y) = a(x, y) + b(x, y)\cos[\varphi(x, y) + pm(x, y)]. \qquad (2)$$

The modulating phase-mask $pm(x,y)$ may have different forms. Millerd et al. [7] and Novak et al. [8] have used the 2x2 building block (or superpixel) shown amplified in Fig. 1. This 2x2 superpixel is periodically repeated all over the CCD to form the phase-mask $pm(x,y)$,

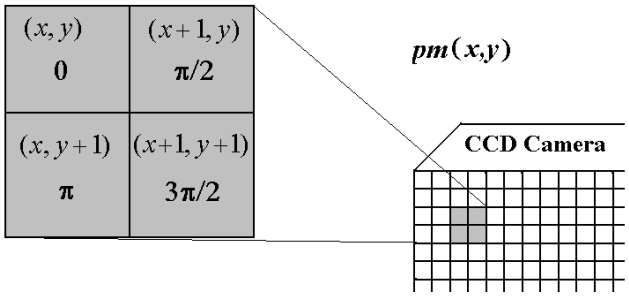

Fig. 1. The basic building block (or superpixel) of the phase-mask proposed in [7,8]. The superpixel is periodically repeated over the entire CCD, giving the spatially homogeneous two dimensional carrier $pm(x,y)$ required by Eq. (2).

We can sort all the 0 degrees pixels to form a continuous 0-degree phase-shifted interferogram. The same is done for the other angles to obtain the 4 phase-shifted interferograms shown in Fig. 2.

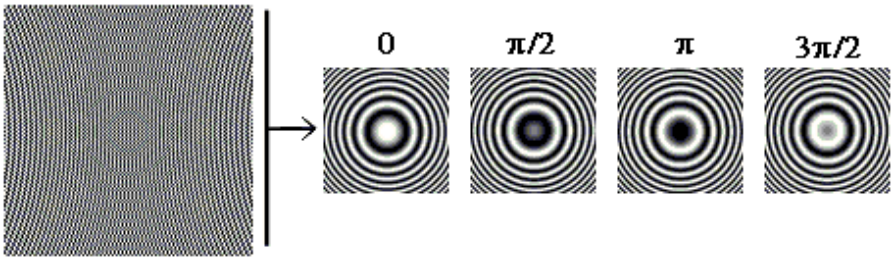

Fig. 2. Four phase-shifted interferograms obtained by sorting the phase-masked CCD pixels according to their phase-shift. The CCD has 2*N*x2*N* pixels, and the four smaller interferograms have *N*x*N* pixels.

As the expert eye would immediately see, one may use a very popular 4-step phase shifting algorithm [1] to estimate the modulating phase at each superpixel's location. Assuming that the modulating phase varies little within the 2x2 superpixel (see Fig. 1). This 4-steps PSI algorithm [7,8] gives a reasonably good estimate of the superpixel's phase as,

$$\hat{\varphi}(x, y) = \tan^{-1}\left[\frac{I(0) - I(\pi)}{I(\pi/2) - I(3\pi/2)}\right] = \tan^{-1}\left[\frac{I(x, y, 0) - I(x, y+1, \pi)}{I(x+1, y, \pi/2) - I(x+1, y+1, 3\pi/2)}\right]. \qquad (3)$$

The "hat" over the demodulated phase denotes its estimated value which may be a bit different from $\phi(x,y)$. A very important thing to notice is that these 4 pixels are not only

#130068 - $15.00 USD Received 14 Jun 2010; revised 10 Jul 2010; accepted 10 Jul 2010; published 13 Aug 2010

phase-shifted but also *spatially-displaced*. This spatial displacement generates a significant detuning error on the superpixel's estimated phase for fast spatial variations on $\phi(x,y)$. In Fig. 3(a) we show the demodulated phase for a chirped wavefront using Eq. (3), and in Fig. 3(b) its estimated error, $\phi_{error}(x,y)=\hat{\phi}(x,y)-\phi(x,y)$,

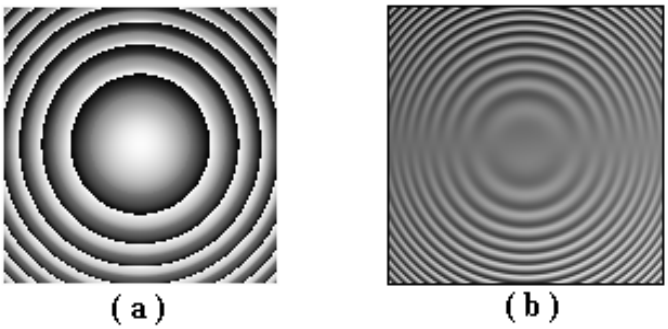

Fig. 3. In panel (a) we show the estimated phase (within $[-\pi,\pi]$) according to Eq. (3), and in panel (b) the phase demodulation error $\phi_{error}(x,y)$ due to the use of this 4-steps algorithm.

The gray-level's contrast in panel 3(b) was multiplied by 5 for displaying purposes (*i.e.* gray-levels within $[-\pi/5,\pi/5]$). This figure shows the typical doubling fringe-pattern phase-error associated with the 4-step algorithm's detuning [1,7–9]. The most important drawbacks of the 4-step demodulation of phase-masked interferograms are,

(a) One looses 3 pixels out of 4 that compose each 2x2 superpixel's building block. However, Millerd et al. [7] comment that Eq. (3) may be used all over the CCD, demodulating almost all its pixels, just as one does with any windowed convolution filter. Unfortunately they have not published the details on how to do it.

(b) The 4-step formula in Eq. (3) is very sensitivity to detuning [1,7–10]. The doubling fringe-pattern phase-error associated with this algorithm is clearly shown in Fig. 3(b).

This detuning error has been analyzed more carefully by Kimbrough [10] along with some higher (9-steps) order algorithms lowering the detuning error. Error-free pixelated interferogram demodulation has however not been achieved and was thought to be difficult.

One way to *absolutely* remedy these two problems is presented in the next section as the general theory for the exact phase demodulation of pixelated interferograms.

2. Error-free demodulation of pixelated carrier interferograms

The general theory behind the error-free phase demodulation of pixelated interferograms is extremely simple yet elegant and mathematically rigorous.

Let us start by observing that in order to *experimentally* generate the interference fringes $I = a + b\cos[\phi + pm]$ in Eq. (2) one would require the following wavefront reference,

$$R(x,y) = \exp[i\ pm(x,y)]. \tag{4}$$

Where $i = (-1)^{1/2}$. This complex reference may in turn be used to demodulate our fringe pattern $I(x,y)$. The first step toward this end is to multiply our interferogram and our reference,

$$I(x,y)R(x,y) = \{\ a(x,y) + b(x,y)\cos[\varphi(x,y) + pm(x,y)]\ \}\exp[i\ pm(x,y)]. \tag{5}$$

The real and imaginary parts of this complex signal are,

$$\begin{aligned} \mathrm{Re}[I(x,y)R(x,y)] &= a\cos(pm) + (b/2)\cos(\varphi + 2pm) + (b/2)\cos(\varphi) \\ \mathrm{Im}[I(x,y)R(x,y)] &= a\sin(pm) + (b/2)\sin(\varphi + 2pm) + (b/2)\sin(\varphi). \end{aligned} \tag{6}$$

#130068 - $15.00 USD Received 14 Jun 2010; revised 10 Jul 2010; accepted 10 Jul 2010; published 13 Aug 2010

Where the operators Re[.] and Im[.] take the real and the imaginary parts of their argument. The two real signals in Eq. (6) are shown in Fig. 4.

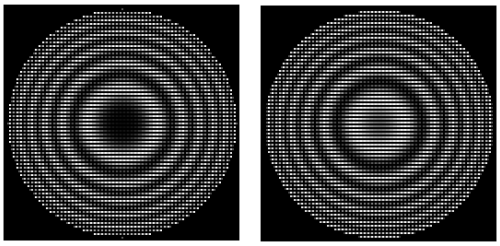

Fig. 4. Here we show the real (in panel (a)) and the imaginary (in panel (b)) signals of the product $I(x,y)R(x,y)$. The function $I(x,y)$ is the measured interferogram in Eq. (2), and the signal $R(x,y)$ is the reference wavefront $\exp[i\, pm(x,y)]$.

Using a narrow-band high-frequency reference $\exp[i\, pm(x,y)]$ one is able to separate the different diffracting orders in Eq. (6). To achieve this spectral separation one needs to keep with the following conditions between $pm(x,y)$ and $\phi(x,y)$,

$$\left|\frac{\partial\, pm(x,y)}{\partial x}\right| > \left|\frac{\partial \varphi(x,y)}{\partial x}\right|_{\max}, \quad and \quad \left|\frac{\partial\, pm(x,y)}{\partial y}\right| > \left|\frac{\partial \varphi(x,y)}{\partial y}\right|_{\max}. \tag{7}$$

Where $|.|_{\max}$ denote the maximum magnitude for $\partial\phi(x,y)/\partial x$ and $\partial\phi(x,y)/\partial y$. If the conditions stated in Eq. (7) are fulfilled, the three signals in Eq. (6) are spectrally separated. We then low-pass filter the signals in Eq. (6) to obtain,

$$\begin{aligned} LPF\left\{\ \mathrm{Re}[I\exp(i\ pm)]\ \right\} &= (b/2)\cos(\varphi) \\ LPF\left\{\ \mathrm{Im}[I\exp(i\ pm)]\ \right\} &= (b/2)\sin(\varphi). \end{aligned} \tag{8}$$

Where $LPF\{.\}$ is a linear low pass filter. Finally the error-free estimated phase is given by the ratio of these two real signals,

$$\hat{\varphi}(x,y) = \tan^{-1}\left\{ \frac{[b(x,y)/2]\sin[\varphi(x,y)]}{[b(x,y)/2]\cos[\varphi(x,y)]} \right\}. \tag{9}$$

The technique just presented may be regarded as the generalization of what is sometimes called the "Direct" interferometric method [1]. But in this case instead of a tilted reference plane one uses a more complicated two dimensional carrier $pm(x,y)$. In the next section we provide two examples of 2x2 superpixels' masks; their spectra and their demodulated phase.

3. Two illustrative examples

Figure 5 graphically shows the proposed demodulation technique applied to a (computer generated) interferogram phase modulated by $pm(x,y)$. Panel 5(a) shows the pixelated interferogram and in panel 5(b) its spectral magnitude. Note that the spectral distance between $b\cos[\phi + pm]$ and the background a is π radians. Panel 5(c) shows the spectrum of the product $I(x,y)\exp[i\, pm(x,y)]$. It is interesting to note in panel 5(c), that the searched complex signal is moved to the spectral origin. A linear low-pass filter selects the centered part of the spectrum shown in panel 5(c); we have implemented the low-pass filter in the Fourier domain. Finally, the error-free demodulated phase is shown wrapped in panel 5(d).

#130068 - $15.00 USD Received 14 Jun 2010; revised 10 Jul 2010; accepted 10 Jul 2010; published 13 Aug 2010

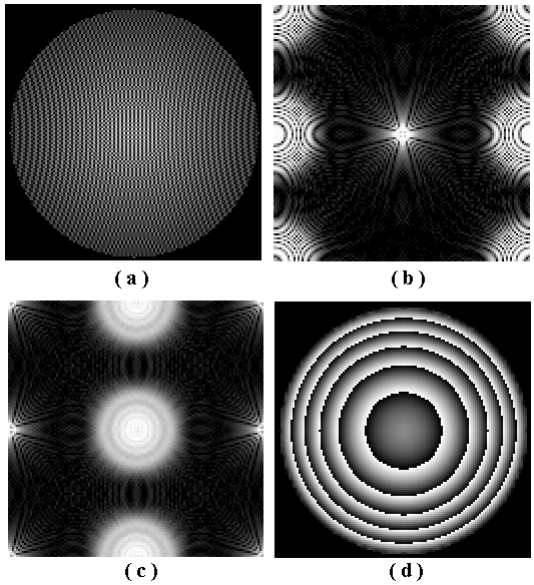

Fig. 5. Phase demodulation of the interferogram $I = a + b\cos[\phi + pm]$, phase modulated by the periodic phase-mask $pm(x,y)$. Panel (a) shows the pixelated interferogram. Panel (b) is the spectrum of the interferogram. Panel (c) shows the spectra of the product $I(x,y)\exp[i\ pm(x,y)]$. Note that the conjugate spectra are separated π radians Finally Panel (d) shows the wrapped (error-free) demodulated phase.

Note that the demodulated phase is error-free as long as their spectra in panel 5(c) remain well separated. Also note that the two information-rich spectra in panel 5(c) are separated a distance of π radians.

Let us continue with a slightly different 2x2 periodic phase-mask. The question is: what would happen if we use the periodic phase-mask shown in Fig. 6 instead of the one in Fig. 1?.

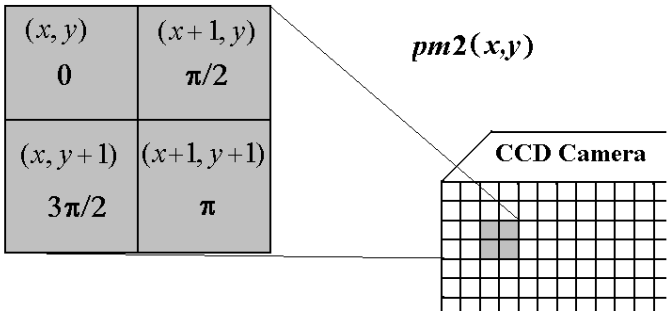

Fig. 6. Another possible phase-mask $pm2(x,y)$ that may be used to modulate the wavefront under measurement.

In Fig. 7 we see the consequences of using the alternative modulating carrier $pm2(x,y)$. Panel 7(a) shows a computer generated pixelated interferogram, and in panel 7(b) we show its spectrum. Panel 7(c) shows the spectra of the product $I(x,y)\exp[i\ pm2(x,y)]$. It is interesting to note in this panel that the searched complex signal $(b/2)\exp[i\ \phi(x,y)]$ is also sent to the spectral origin. We finally keep the centered spectrum by low-pass filtering in the Fourier domain to obtain the error-free demodulated phase shown in panel 7(d).

#130068 - $15.00 USD Received 14 Jun 2010; revised 10 Jul 2010; accepted 10 Jul 2010; published 13 Aug 2010

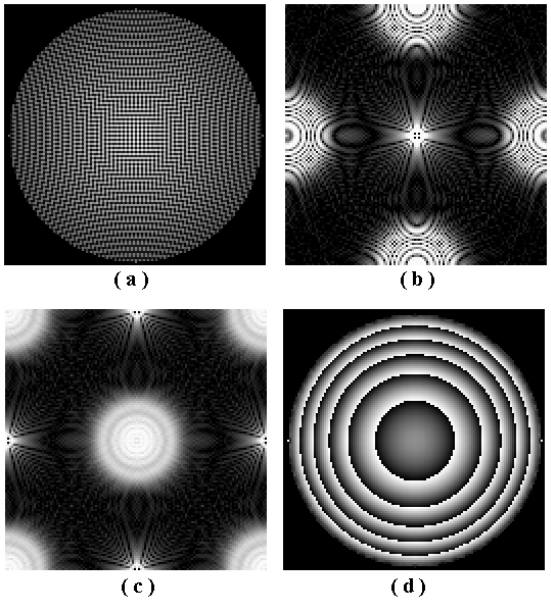

Fig. 7. Phase estimation of the interferogram modulated by $pm2(x,y)$; $I = a + b\cos[\phi + pm2]$. Panel (a) shows the pixelated carrier interferogram. Panel (b) shows the spectrum of the interferogram. Note that the conjugate spectra are separated $(\sqrt{2})\pi$ radians. Panel (c) shows the spectra of the product $I(x,y)\exp[i\ pm2(x,y)]$. And finally Panel (d) shows the wrapped (error-free) demodulated phase.

As before, the demodulated phase in panel 7(d) is error-free as long as the centered spectra in panel 7(c) (signal in Eq. (8)) remain well separated from the other spectral components. Also the modulating phase was estimated all over the entire CCD's pixels.

Note that, phase detuning error arises because some undesired signal from the conjugate spectrum leaks into the desired analytical signal [9]. In our method this is not possible because we have filtered-out completely this conjugate spectrum in the Fourier domain.

Also note that the spectral distance between the two conjugate spectra in panel 7(c) is $(\sqrt{2})\pi$ radians, while this separation in panel 5(c) due to $pm(x,y)$ is π radians. This means that the spectral space is more efficiently used modulating by $pm2(x,y)$ rather than by $pm(x,y)$. Moreover, the spectral distance between the pixelated carrier and its two conjugate spectra are π radians. Pixelated carriers use the available spectral space more efficiently than a reference plane, because pixelated carriers have two-dimensional degrees of freedom, while a tilted reference are confined to a single dimension (a line in the plane).

4. Conclusions

We have presented a very easy, yet efficient and straightforward method to demodulate the phase of pixelated spatial-carrier interferograms without detuning error. As far as we know, demodulating pixelated phase-masked interferograms with no detuning error and without discarding valuable CCD pixels has not been reported before. We have presented two alternative phase modulating masks $pm(x,y)$ and $pm2(x,y)$ with good results graphically shown in Figs. 5 and 7. Finally we have driven the reader's attention to the high efficient use of the available spectral space by the pixelated carriers reviewed in this paper. The spatial phase carrier $pm2(x,y)$ separate the information-rich conjugate spectra a distance of $(\sqrt{2})\pi$ radians, while the $pm(x,y)$ carrier separate them only π radians. In turn these two carrier masks use more efficiently the available spectral space than a single dimension carrier obtained by tilting a reference plane.

#130068 - $15.00 USD Received 14 Jun 2010; revised 10 Jul 2010; accepted 10 Jul 2010; published 13 Aug 2010